Deep-Sea Research, Vol. 36, No. 1, pp. 39–53, 1989.
Printed in Great Britain.

0198–0149/89 $3.00 + 0.00

On the size of the Antarctic Circumpolar Current

GREGORY C. JOHNSON* and HARRY L. BRYDEN†

(*Received 7 March* 1988; *in revised form* 17 *August* 1988; *accepted* 19 *August* 1988)

Abstract—A model predicted transport of the Antarctic Circumpolar Current (ACC) through Drake Passage compares favorably with measured transport through the passage. The model incorporates the width of the ACC, the strong eddy presence in the region, and the deep penetration of an unstable baroclinic velocity field, all of which are characteristic features of the current. The model involves a downward transfer of wind-imparted zonal momentum by eddy form drag to a depth at which it can be removed by bottom pressure drag. The eddy form drag results from a poleward transport of heat by eddies originating from the baroclinically unstable current.

The problem: what sets the size of the ACC?

Stommel 1957, 1962: Early models adapt Sverdrup dynamics to the ACC, relating wind stress curl to transport.

Munk and Palmen, 1951: Such models require ‘uncomfortably large’ values of eddy friction coefficients to limit the ACC transport to reasonable values.

Gill 1968: Linear model of the ACC requires a bottom friction coefficent of 10^3 cm^2/s
a lateral friction coefficient of 10^8 cm^2/s.

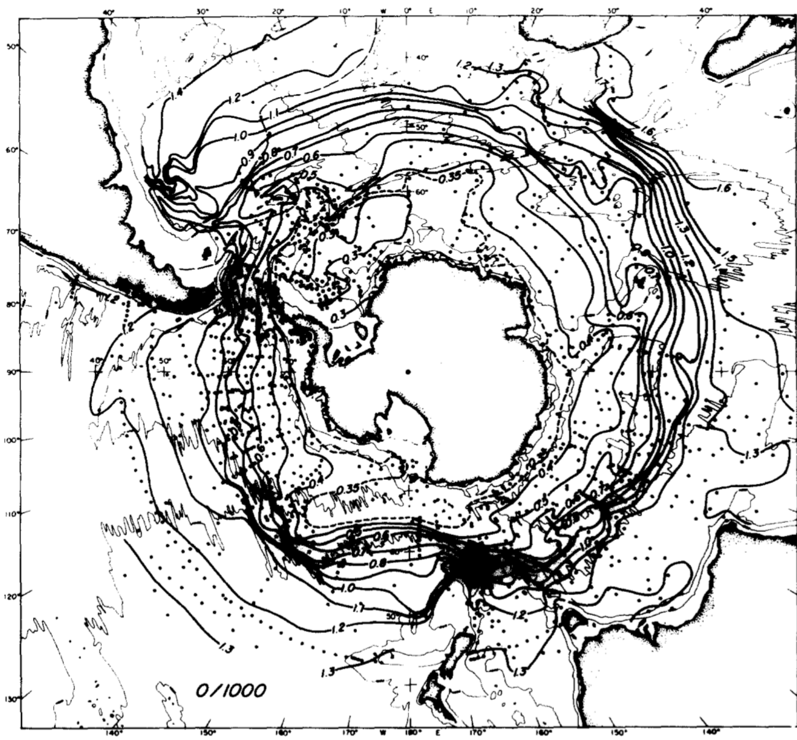

Fig. 1. 0–1000 db dynamic height field of the Southern Ocean in dynamic meters with 4000 m isobath and station locations. Figure 2 from GORDON *et al.* (1978).

The problem: what sets the size of the ACC?

Stommel 1957, 1962: Early models adapt Sverdrup dynamics to the ACC, relating wind stress curl to transport.

Munk and Palmen, 1951: Such models require ‘uncomfortably large’ values of eddy friction coefficients to limit the ACC transport to reasonable values.

Gill 1968: Linear model of the ACC requires a bottom friction coefficent of 10^3 cm^2/s
a lateral friction coefficient of 10^8 cm^2/s.

Even worse: how big *is* the ACC?

Reid and Nowlin, 1971: Eastward transport of 237 Sv through the Drake Passage

Foster, 1972: **Westward** transport of 15 Sv through the Drake Passage (backwards!)

International Southern Ocean Studies (ISOS) program measures Drake Passage transport, structure, dynamics.

Nowlin and Klinck, 1986: 134 Sv +- 10% (eastward), with time variability of 20%.

Nowlin and Klinck, 1986: 134 Sv +- 10% (eastward), with time variability of 20%.

ACC characteristics:

- NOT a narrow jet or boundary current with with Ro
- Three narrow frontal regions of width two or three times the Rossby radius
- The current penetrates down to the bottom of the water column, with substantial meridional density gradients at depth.

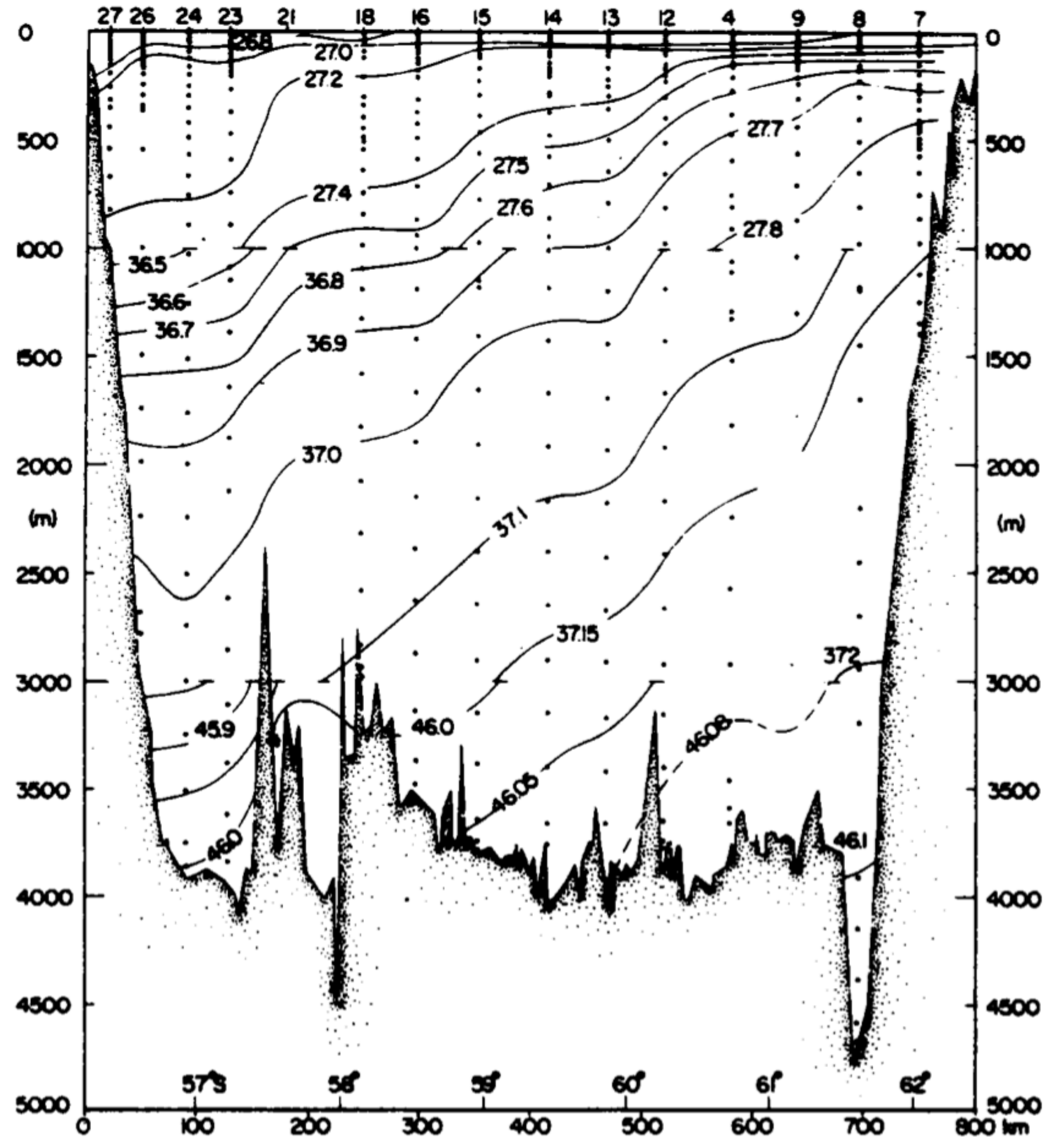

Fig. 2. Section of variability referenced density parameter σ across Drake Passage calculated from *Melville* Section II FDRAKE 75 data. Figure 4 from NOWLIN *et al.* (1977).

McWilliams et al., 1978: A 2-layer, eddy-resolving QG model of the ACC with various configurations of topography and wind forcing.

In all model runs, eddies played a key role in transporting zonal momentum downward.

In model runs without topography, friction was only strong enough to hold model transport values around 400-600 Sv.

In model runs with topography, topographic form drag was strong enough to limit the model transport to 100 Sv.

Bottom and sidewall friction is not enough! Thus:

The goal of this paper is to present a simple model of the dynamics of the ACC that predicts a transport independent of friction coefficients.

Steady state zonal momentum balance:

$$u\frac{\partial u}{\partial x} + v\frac{\partial u}{\partial y} + w\frac{\partial u}{\partial z} = -\frac{1}{\rho_0}\frac{\partial p}{\partial x} + fv + \frac{1}{\rho_0}\frac{\partial \tau^x}{\partial z} \qquad \text{(eqn 1)}$$

Noting that: $u\frac{\partial u}{\partial x} = \frac{\partial}{\partial x}(uu) - u\frac{\partial u}{\partial x}$ and $\nabla \cdot \mathbf{u} = 0$

$$v\frac{\partial u}{\partial y} = \frac{\partial}{\partial y}(uv) - u\frac{\partial v}{\partial x}$$

$$w\frac{\partial u}{\partial z} = \frac{\partial}{\partial z}(uw) - u\frac{\partial w}{\partial z}$$

We can write eqn (1) as

$$\frac{\partial}{\partial x}(uu) + \frac{\partial}{\partial y}(uv) + \frac{\partial}{\partial z}(uw) = -\frac{1}{\rho_0}\frac{\partial p}{\partial x} + fv + \frac{1}{\rho_0}\frac{\partial \tau^x}{\partial z}$$

Taking the vertical integral:

$$\int_{z=-H}^{0}\left[\frac{\partial}{\partial x}(uu)+\frac{\partial}{\partial y}(uv)+\frac{\partial}{\partial z}(uw)\right]dz=\int_{z=-H}^{0}\left[fv-\frac{1}{\rho_0}\frac{\partial p}{\partial x}+\frac{1}{\rho_0}\partial\tau^x\partial z\right]dz$$

$$\int_{z=-H}^{0}\left[\frac{\partial}{\partial x}(uu)+\frac{\partial}{\partial y}(uv)+\frac{\partial}{\partial z}(uw)\right]dz=$$

$$\frac{\partial}{\partial x}\int_{z=-H}^{0}uudz-(uu)\Big|_{z=-H}\frac{\partial H}{\partial x}$$

$$+\frac{\partial}{\partial y}\int_{z=-H}^{0}uvdz-(uv)\Big|_{z=-H}\frac{\partial H}{\partial y}$$

$$+(uw)\Big|_{z=-H}$$

$$\oint \mathrm{d}x\left[\frac{\partial}{\partial x}\int_{z=-H}^{0}\mathrm{d}z(uu)+\frac{\partial}{\partial y}\int_{z=-H}^{0}\mathrm{d}z(uv)=\int_{0}^{-H}\mathrm{d}z\left(fv-\frac{1}{\rho_0}\frac{\partial p}{\partial x}+\frac{1}{\rho_0}\frac{\partial\tau^x}{\partial z}\right)\right], \qquad (1)$$

Taking the vertical integral:

$$\int_{z=-H}^{0}\left[\frac{\partial}{\partial x}(uu)+\frac{\partial}{\partial y}(uv)+\frac{\partial}{\partial z}(uw)\right]dz=\int_{z=-H}^{0}\left[fv-\frac{1}{\rho_0}\frac{\partial p}{\partial x}+\frac{1}{\rho_0}\partial\tau^x\partial z\right]dz$$

$$\int_{z=-H}^{0}\left[\frac{\partial}{\partial x}(uu)+\frac{\partial}{\partial y}(uv)+\frac{\partial}{\partial z}(uw)\right]dz=$$

$$\frac{\partial}{\partial x}\int_{z=-H}^{0}uudz-\cancel{(uu)\Big|_{z=-H}\frac{\partial H}{\partial x}}$$

$$+\frac{\partial}{\partial y}\int_{z=-H}^{0}uvdz-\cancel{(uv)\Big|_{z=-H}\frac{\partial H}{\partial y}}$$

$$\cancel{+(uw)\Big|_{z=-H}}$$

$$\oint \mathrm{d}x\left[\frac{\partial}{\partial x}\int_{z=-H}^{0}\mathrm{d}z(uu)+\frac{\partial}{\partial y}\int_{z=-H}^{0}\mathrm{d}z(uv)=\int_{0}^{-H}\mathrm{d}z\left(fv-\frac{1}{\rho_0}\frac{\partial p}{\partial x}+\frac{1}{\rho_0}\frac{\partial \tau^x}{\partial z}\right)\right], \qquad (1)$$

In the circumpolar region of the Southern Ocean, integrated zonal momentum balance becomes:

$$\oint \mathrm{d}x \left[\frac{\partial}{\partial y}\int_{z=-H}^{0} \mathrm{d}z(uv) + \int_{z=-H}^{0} \mathrm{d}z \, \frac{1}{\rho_0}\frac{\partial p}{\partial x}\right] = \frac{1}{\rho_0}\oint \mathrm{d}x\tau^x \Big]_{bottom}^{surface} \qquad (2)$$

Momentum source: Frictional wind stress at the surface of the fluid

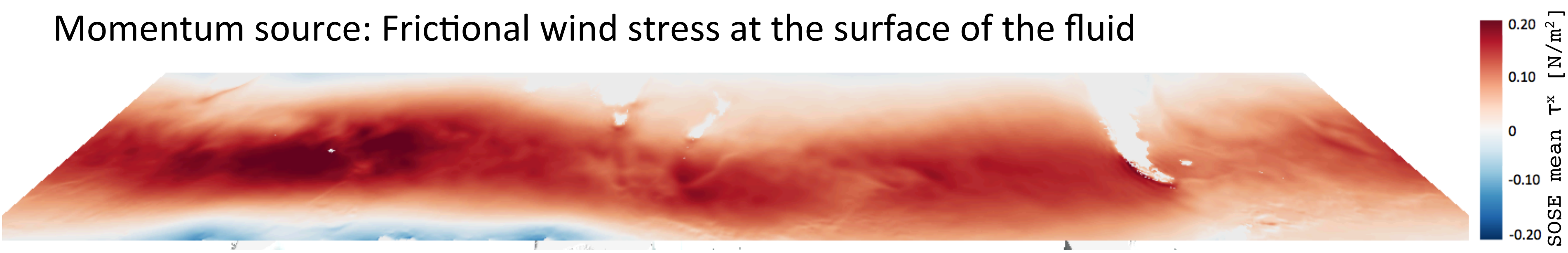

In the circumpolar region of the Southern Ocean, integrated zonal momentum balance becomes:

$$\oint \mathrm{d}x \left[\frac{\partial}{\partial y}\int_{z=-H}^{0} \mathrm{d}z(uv) + \int_{z=-H}^{0} \mathrm{d}z \,\frac{1}{\rho_0}\frac{\partial p}{\partial x}\right] = \frac{1}{\rho_0}\oint \mathrm{d}x\,\tau^x \Big]_{bottom}^{surface} \qquad (2)$$

Momentum source: Frictional wind stress at the surface of the fluid

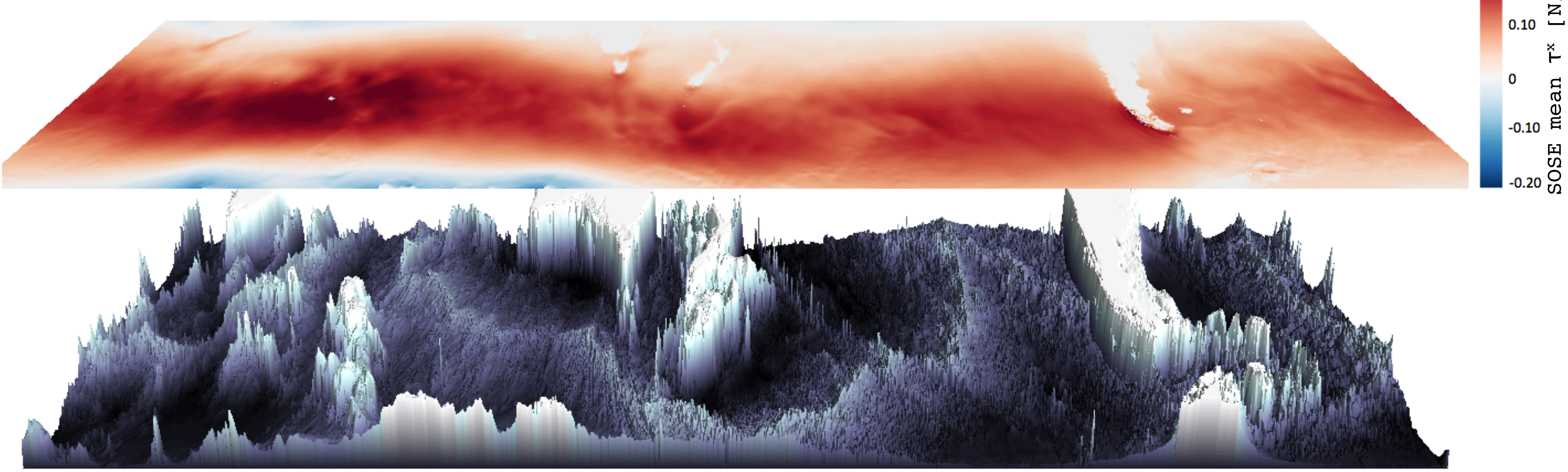

Potential momentum sinks:

1) Frictional stress at the bottom;

In the circumpolar region of the Southern Ocean, integrated zonal momentum balance becomes:

$$\oint \mathrm{d}x \left[\frac{\partial}{\partial y} \int_{z=-H}^{0} \mathrm{d}z(uv) + \int_{z=-H}^{0} \mathrm{d}z \, \frac{1}{\rho_0} \frac{\partial p}{\partial x} \right] = \frac{1}{\rho_0} \oint \mathrm{d}x \tau^x \Big]_{bottom}^{surface} \quad (2)$$

Momentum source: Frictional wind stress at the surface of the fluid

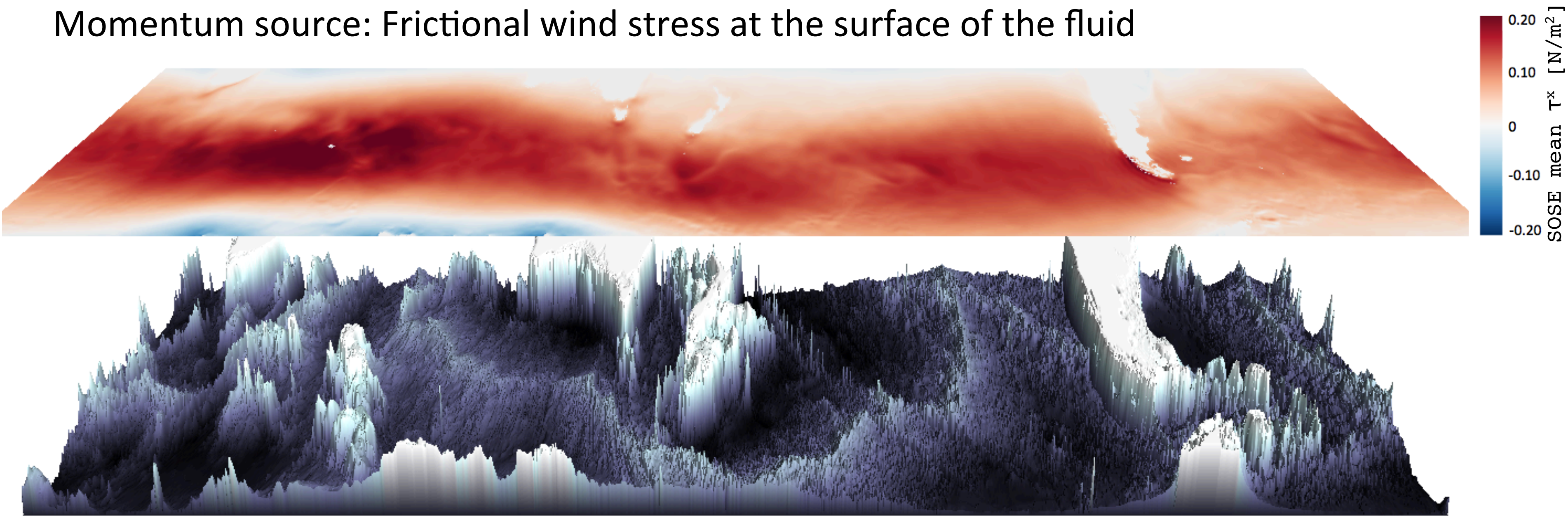

Potential momentum sinks:

1) Frictional stress at the bottom;
2) Frictional stress at the sidewalls, via meridional momentum flux divergence;

In the circumpolar region of the Southern Ocean, integrated zonal momentum balance becomes:

$$\oint \mathrm{d}x \left[\frac{\partial}{\partial y} \int_{z=-H}^{0} \mathrm{d}z(uv) + \int_{z=-H}^{0} \mathrm{d}z \frac{1}{\rho_0} \frac{\partial p}{\partial x} \right] = \frac{1}{\rho_0} \oint \mathrm{d}x \tau^x \Big]_{bottom}^{surface} \tag{2}$$

Momentum source: Frictional wind stress at the surface of the fluid

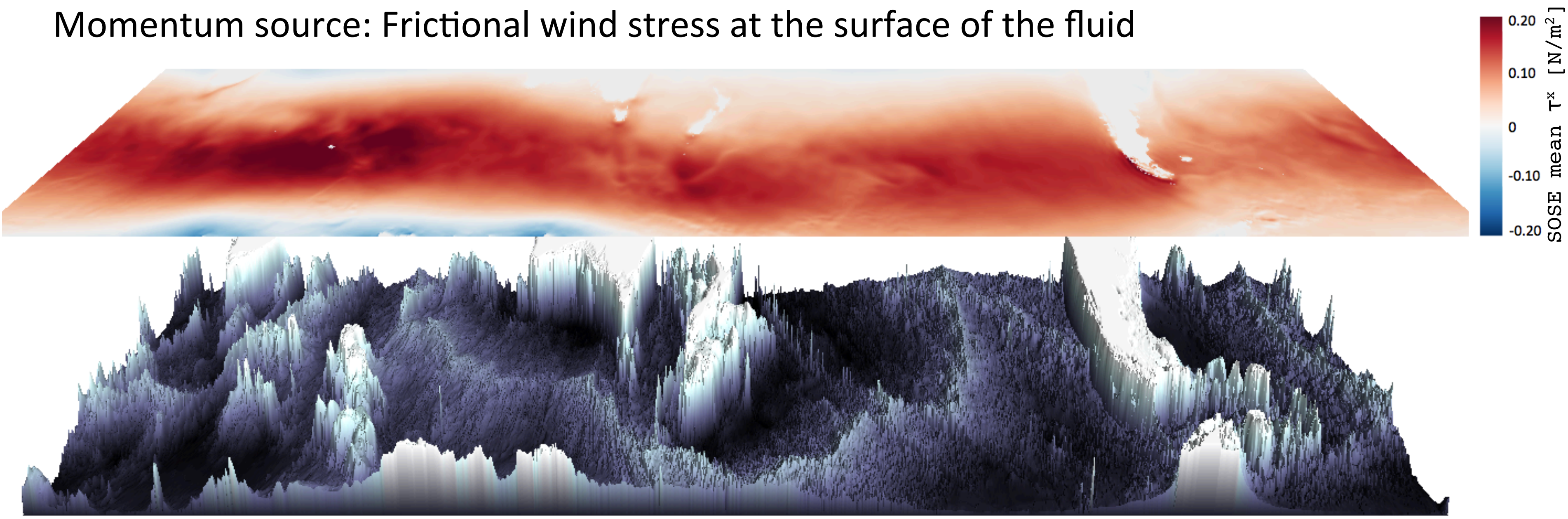

Potential momentum sinks:

1) Frictional stress at the bottom;
2) Frictional stress at the sidewalls, via meridional momentum flux divergence; or
3) Topographic form stress.

Topographic form stress

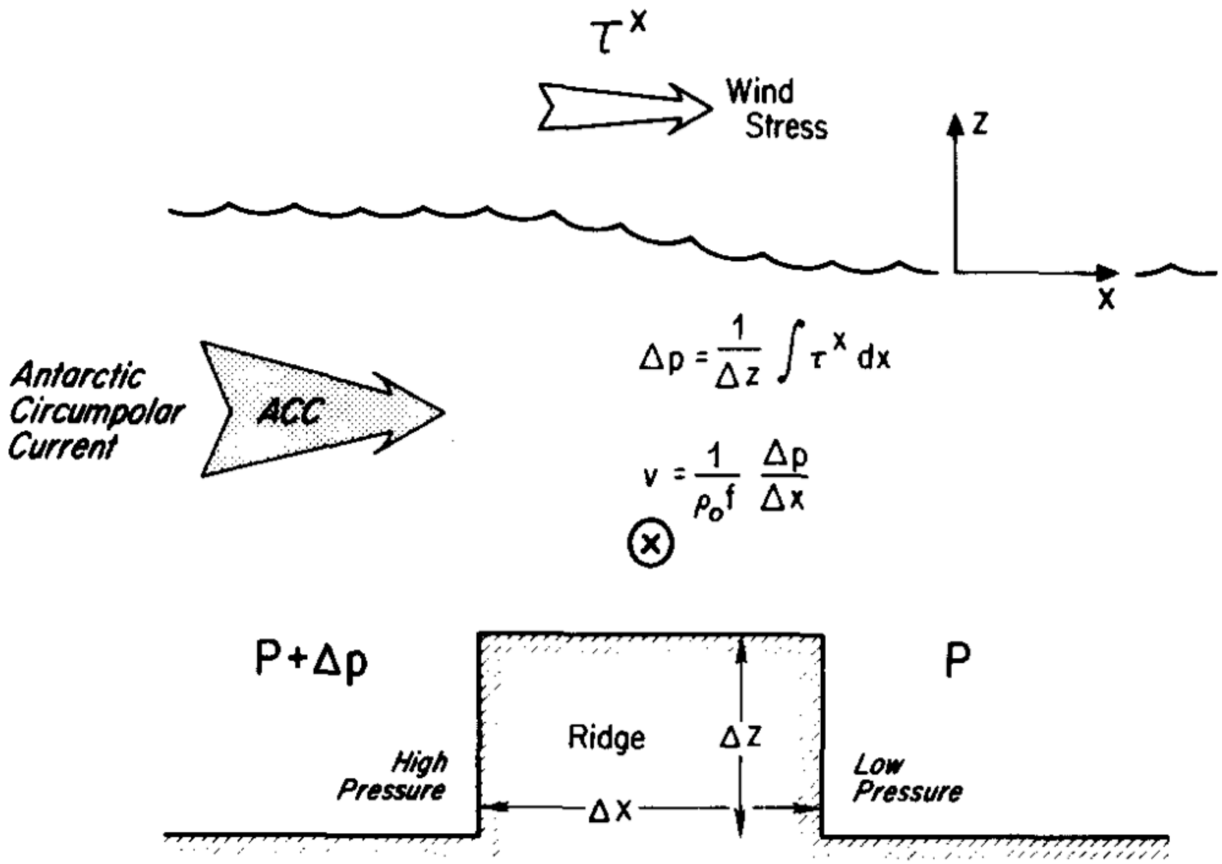

Fig. 3. Schematic presentation of bottom form drag or mountain drag. Wind stress imparted eastward momentum in the water column is removed by the pressure difference across the ridge. Note that geostrophic balance $\rho_0 f v = \partial p/\partial x$ demands an equatorward flow (symbolized by ⊗) along the ridge, evidence of which may be seen in Fig. 1.

How does momentum travel from surface source to seafloor sink?
Interfacial form stress.

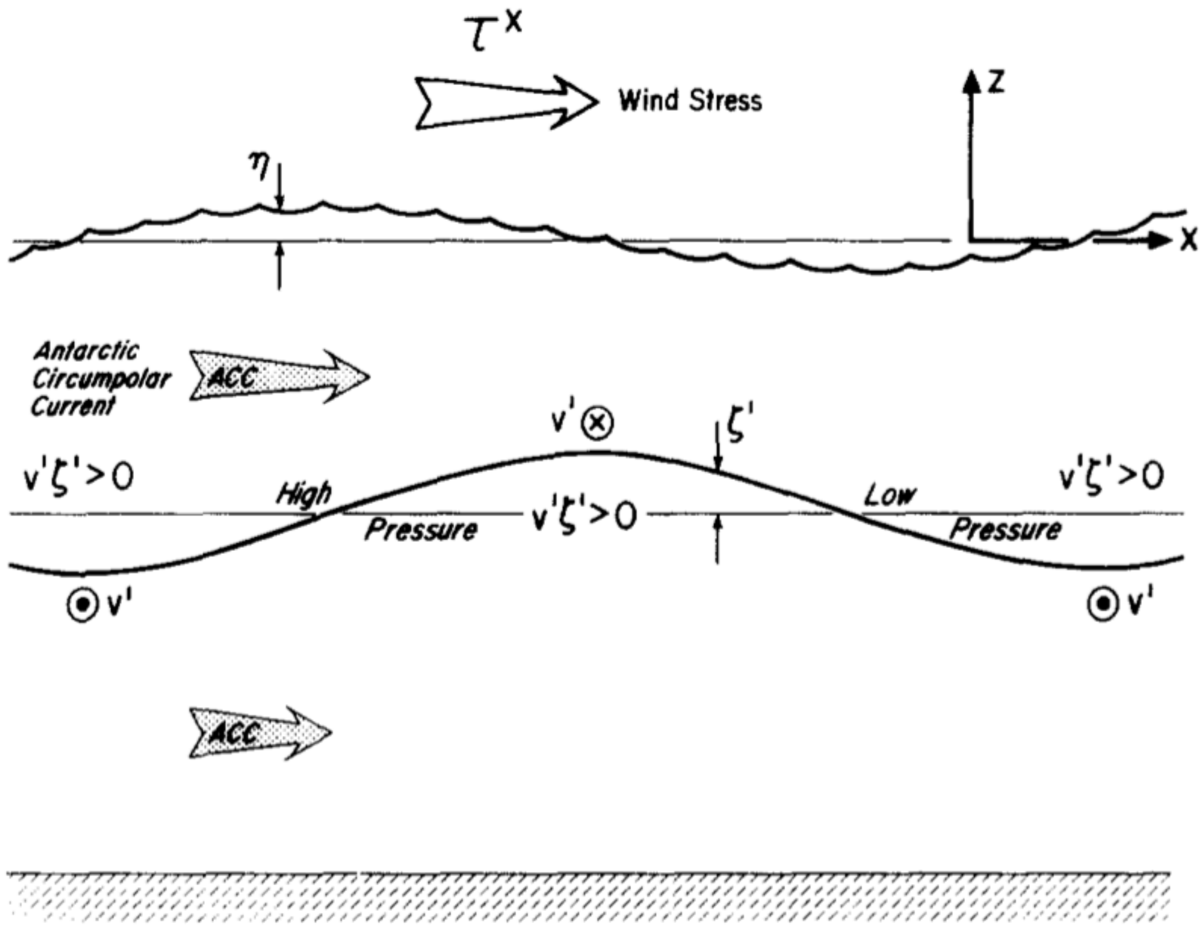

Fig. 4. Schematic presentation of interfacial form drag. Correlations of perturbations in the interface height, ζ', and the meridional velocity, V' ($\odot$ indicating poleward flow and $\otimes$ indicating equatorward flow), which are related to pressure perturbations by geostrophy, allow the upper layer to exert an eastward force on the lower layer and the lower layer to exert a westward force on the upper layer; thus effecting a downward flux of zonal momentum.

How does momentum travel from surface source to seafloor sink?
Interfacial form stress.

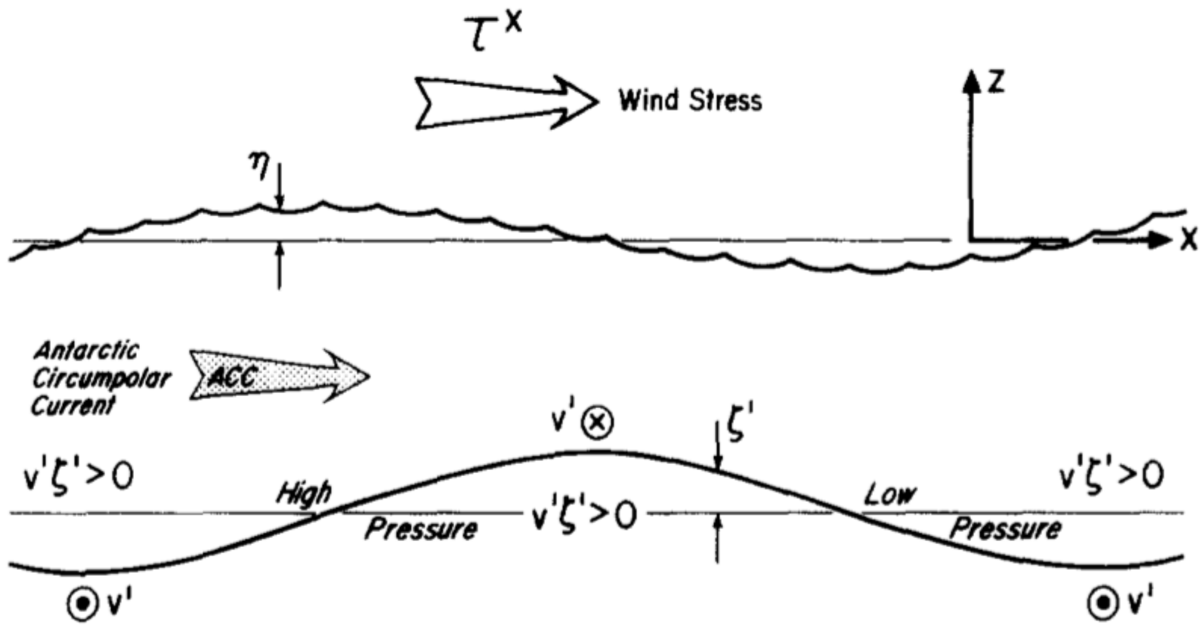

$$\oint p' \frac{\partial \zeta'}{\partial x}\,\mathrm{d}x = -\oint \zeta' \frac{\partial p'}{\partial x}\,\mathrm{d}x = \oint f \frac{\overline{v'T'}}{\overline{\theta}_z}\,\mathrm{d}x$$

continuous stratification

$$\zeta' = -\frac{T'}{\overline{\theta}_z}$$

and

geostrophy

$$\frac{1}{\rho_0}\frac{\partial p'}{\partial x} = f v'$$

$$\oint p' \frac{\partial \zeta'}{\partial x}\,\mathrm{d}x = -\oint \zeta' \frac{\partial p'}{\partial x}\,\mathrm{d}x = \oint f \frac{\overline{v'T'}}{\overline{\overline{\theta}}_z}\,\mathrm{d}x$$

Interfacial form stress:

Vertical flux of eastward momentum is proportional to eddy heat flux.

Poleward heat flux corresponds to the downward flux of eastward momentum.

THE MODEL

$$\rho_0 f \frac{\overline{v'T'}}{\overline{\theta}_z} = \tau^x \qquad \forall z$$

downward eddy flux of eastward momentum $=$ wind stress at all depths.

Given a few numbers…

$$\rho_0 = 1030 \text{ kg/m}^{\,3}$$

$$f = -1.25 \times 10^{-4} \text{ 1/sec}$$

$$\tau^x \big|^{surface} = 2 \text{ N/m}^{\,2}$$

….this model can be tested observationally.

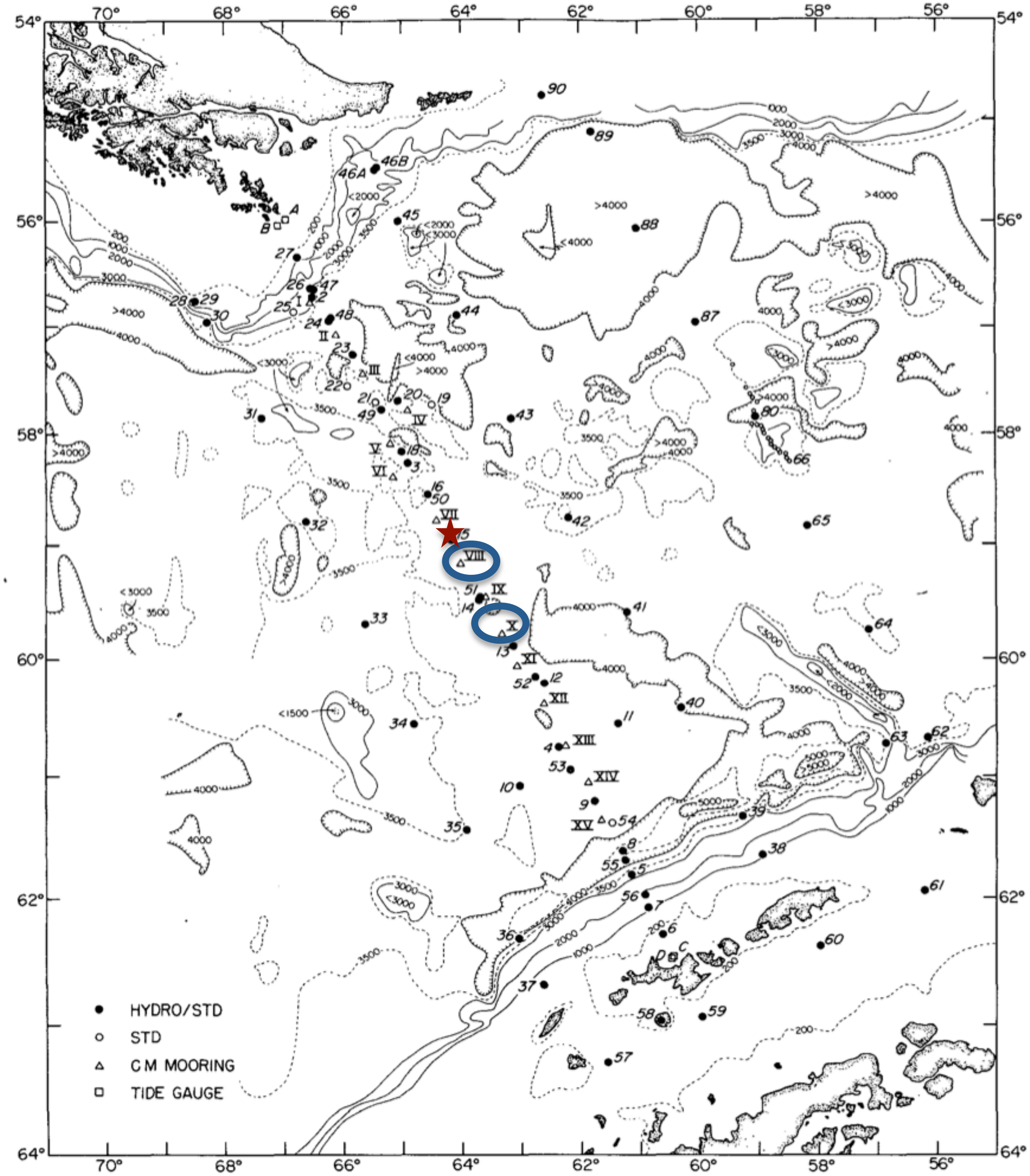

FIG. 1. *Melville* station plan, FDRAKE 75, 19 February–30 March 1975.

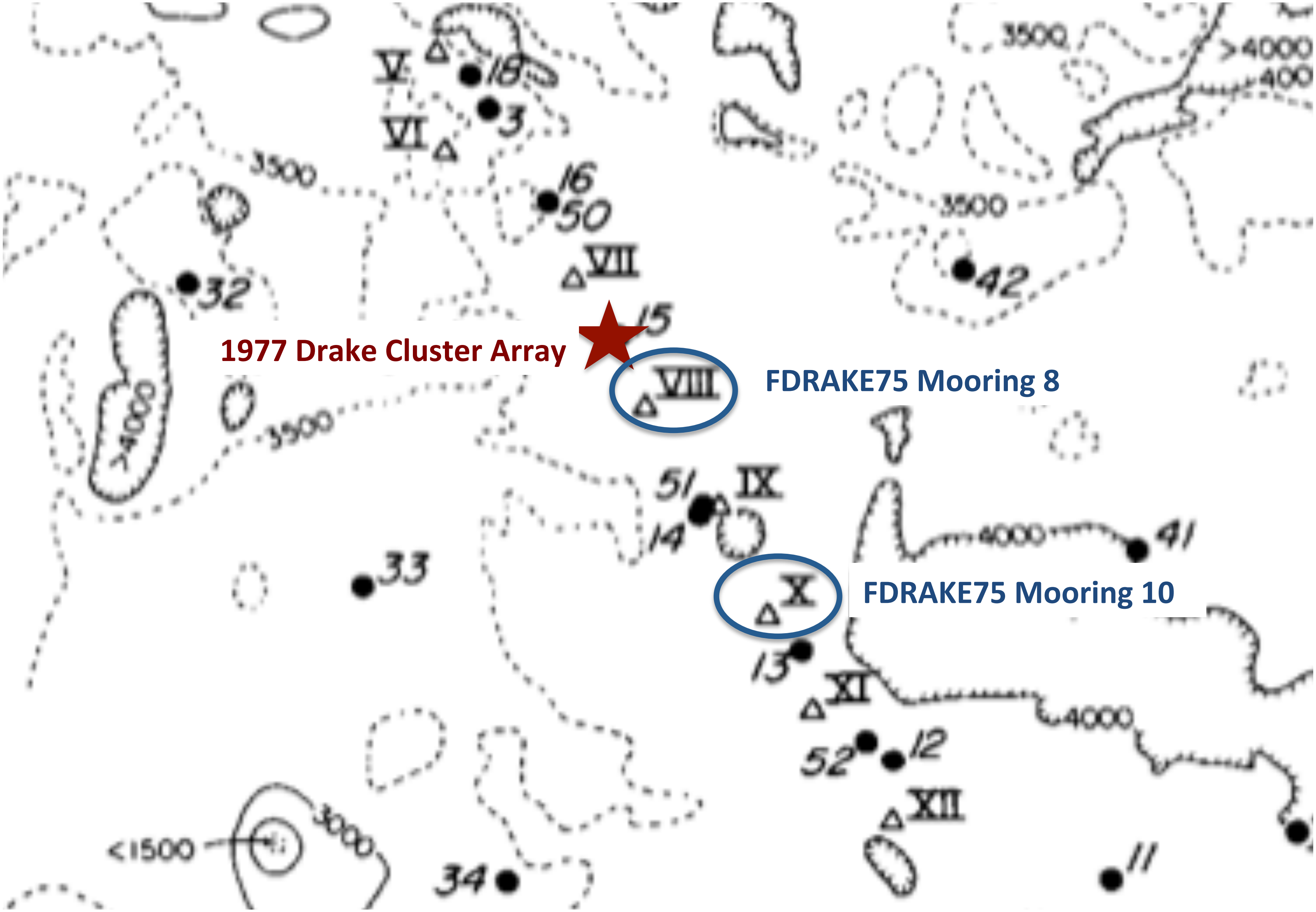
1977 Drake Cluster Array
FDRAKE75 Mooring 8
FDRAKE75 Mooring 10
V
VI
VII
VIII
IX
X
XI
XII
18
3
16
50
32
15
42
51
14
41
33
13
52
12
34
11
3500
3500
3500
3500
>4000
4000
4000
4000
3000
<1500

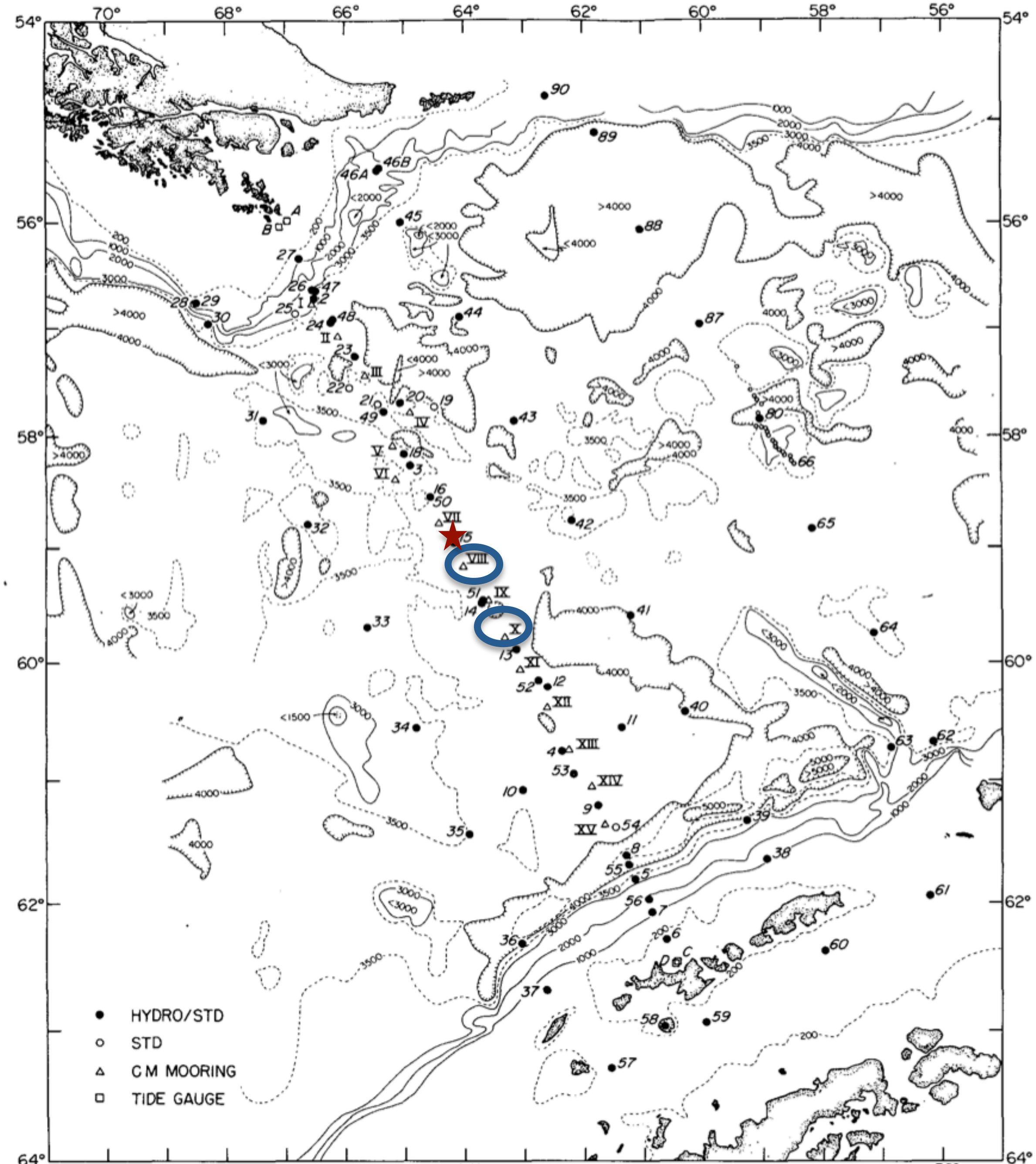

FIG. 1. *Melville* station plan, FDRAKE 75, 19 February–30 March 1975.

Observations used to test $\overline{v'T'} = \frac{1}{\rho_0 f} \tau^x \overline{\theta_z}$

Table 1. *Eddy heat flux and downward momentum flux for current meter records in central Drake Passage. Data used were taken in Drake Passage during the ISOS program. Current meter data used to calculate eddy heat flux values is taken from the* 1977 *central Drake Passage Cluster Array at* 59°S, 64°W (BRYDEN, 1979b), *and moorings* 8 (59°S, 64°30′W) *and* 10 (60°S, 63°W) *from the FDRAKE* 75 *mooring array. Calculation of* $\overline{\theta_z}$ *was performed using an arithmetic mean of hydrographic/STD stations* 13, 14, 15, 33 *and* 42 *taken near the moorings by the R.V.* Melville *during FDRAKE* 75. *Values of* $\rho_0 = 1.03$ g cm^{-3} *and* f = -1.25×10^{-4} s^{-1} *(appropriate for* 59°S) *were used. See* NOWLIN et al. (1977) *Fig.* 1, *for locations of R.V.* Melville *stations and moorings* 8 *and* 10

Depth (m)	Eddy heat flux $\overline{V'T'}$ (°C cm s^{-1})	Vertical temperature gradient $\overline{\theta_z}$ (× 10^{-4} °C cm^{-1})	Downward momentum flux $\rho_0 f\ \overline{V'T'}/\overline{\theta_z}$ (dyn cm^{-2})
580*	−0.39	0.066	7.6
1020†	−0.33	0.056	7.6
1100*	−0.36	0.056	8.3
1520†	−0.32§	0.079	5.2
2080*	−0.34§	0.074	5.9
2520†	−0.24§	0.079	3.9
2750‡	−0.20	0.074	3.5
3560*	−0.18	0.054	4.3

* 1977 Drake Passage Cluster Array Moorings.
† FDRAKE 75 mooring 10.
‡ FDRAKE 75 mooring 8.
§ Significantly different from zero at the 95% confidence level.

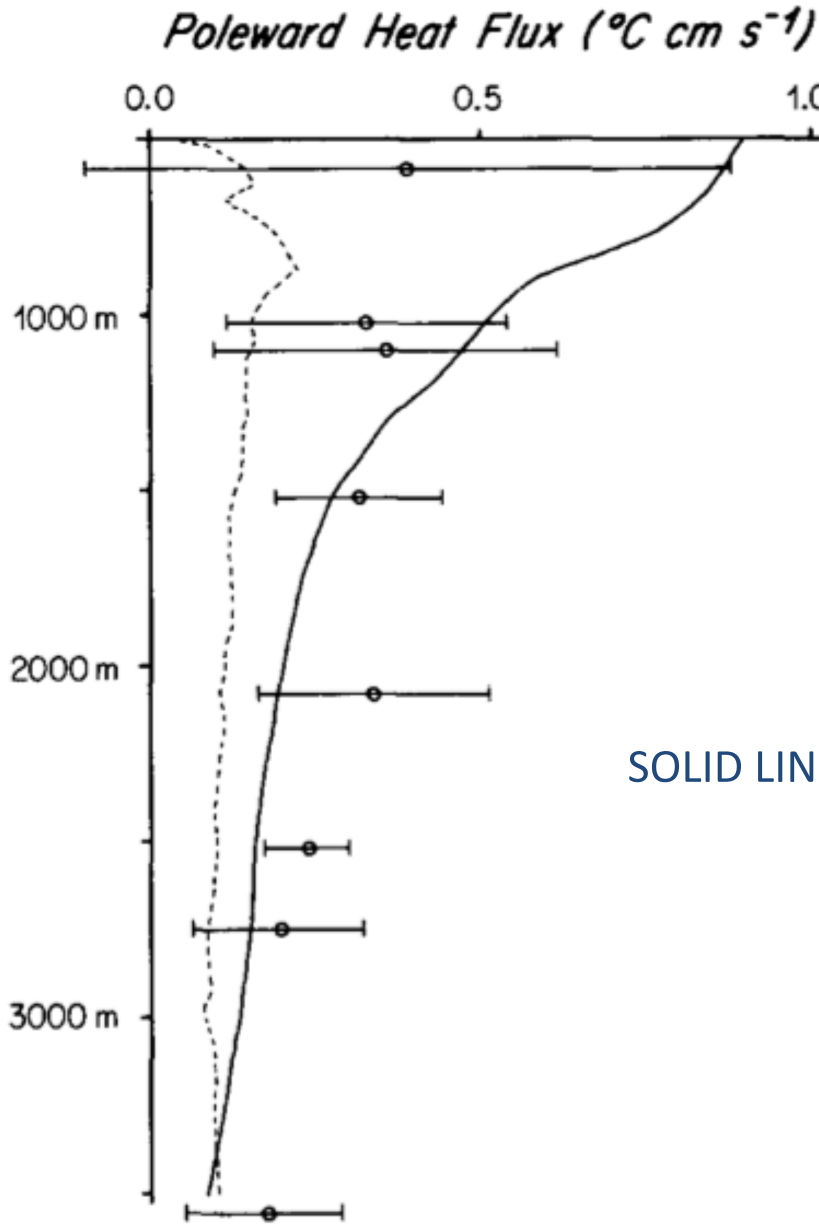

SOLID LINE $\overline{v'T'} = \frac{1}{\rho_0 f}\tau^x\overline{\theta_z}$

Fig. 5. Measured eddy heat flux in central Drake Passage (discrete points with standard error bars) plotted with eddy heat flux predicted from a momentum flux balance argument (equation (4), dashed line) and a large-scale baroclinic field parameterization (equation (5), solid line).

Second test:
Can down-gradient eddy heat flux be parameterized in terms of time-averaged baroclinic fields a la Green (1970) and Stone (1972)?

$$V' \propto H\overline{U_z}$$

$$T' \propto \pi R_0 \overline{T_y}$$

$$\overline{V'T'} = CH\pi R_0 \overline{U_z}\,\overline{T_y}$$

where
H is the water depth,
$R_0 = \frac{1}{\pi f_0} \int_{z=-H}^{z=0} N(z)dz$ is the Rossby radius,
$\overline{U_z}$ is the vertical shear of the time averaged u field,
$\overline{T_y}$ is the large-scale meridional temperature gradient, and
C is the correlation coefficient between velocity and temperature fluctuations.

Employing the thermal wind balance $\rho_0 \overline{fU_z} = g\alpha\overline{T_y}$, where g is gravity and $\alpha = \frac{d\rho}{dT}$, the eddy heat flux term becomes:

$$\overline{V'T'} = CH\pi R_0 \frac{\rho_0 f_0}{g\alpha} \overline{U_z^2}.$$

Observations used to test $\overline{V'T'} = C H \pi R_0 \frac{\rho_0 f_0}{g\alpha} \overline{U_z^2}$.

Table 2. Test of Stone's eddy heat flux parameterization for Drake Passage current meter and hydrographic data. The source for eddy heat flux values is documented in Table 1. *A value of* 3500 m *was chosen for the depth of the passage* H. *The Rossby radius* R_0 *was calculated using an* N^2 *constructed from an arithmetic mean of hydrographic/STD stations* 8, 9, 4, 12, 14, 15, 16, 18, 20, 23 *and* 24 *taken by R.V.* Melville *and spanning the passage (see Table* 1 *for details). Calculations of* $\overline{U_z}$ *and* $\overline{T_y}$ *were performed with deep end stations* 8 *and* 24

Depth (m)	Eddy heat flux $\overline{V'T'}$ (°C cm s^{-1})	Large-scale scaled baroclinic shear fields $H\pi R_0\overline{U_z T_y}$(°C cm s^{-1})	Correlation coefficient $C = \overline{V'T'}/H\pi R_0\overline{U_z T_y}$
580*	–0.39	6.35	0.06
1020†	–0.33	3.73	0.09
1100*	–0.36	3.39	0.11
1520†	–0.32§	2.04	0.16
2080*	–0.34§	1.37	0.25
2520†	–0.24§	1.12	0.21
2750‡	–0.20	1.09	0.18
3560*	–0.18	0.56	0.32

* 1977 Drake Passage Cluster Array Moorings.
† FDRAKE 75 mooring 10.
‡ FDRAKE 75 mooring 8.
§ Significantly different from zero at the 95% confidence level.

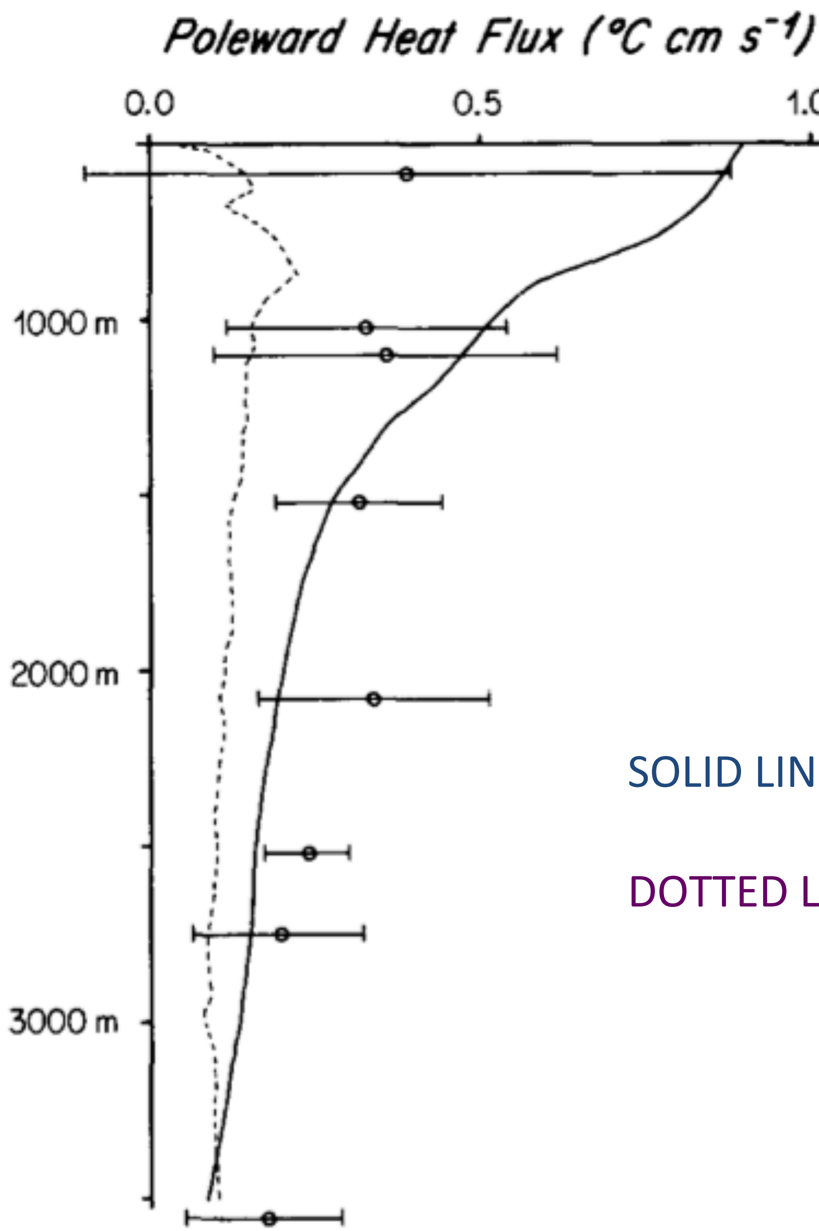

SOLID LINE $\overline{v'T'} = \frac{1}{\rho_0 f}\tau^x \overline{\theta_z}$

DOTTED LINE $\overline{V'T'} = CH\pi R_0 \frac{\rho_0 f_0}{g\alpha} \overline{U_z^2}$

Fig. 5. Measured eddy heat flux in central Drake Passage (discrete points with standard error bars) plotted with eddy heat flux predicted from a momentum flux balance argument (equation (4), dashed line) and a large-scale baroclinic field parameterization (equation (5), solid line).

Estimating transport

SOLID LINE $\overline{v'T'} = \frac{1}{\rho_0 f} \tau^x \overline{\theta_z}$

DOTTED LINE $\overline{V'T'} = CH\pi R_0 \frac{\rho_0 f_0}{g\alpha} \overline{U_z^2}$

Estimating transport:

Setting eddy heat flux estimates equal to each other:

$$\frac{1}{\rho_0 f}\tau^x\overline{\theta_z} = CH\pi R_0 \frac{\rho_0 f_0}{g\alpha}\overline{U_z^2}.$$

Allows us to calculate time averaged ACC vertical shear:

$$\overline{U_z}(z) = \frac{N(z)}{f}\sqrt{\frac{\tau_x}{\rho_0 CH\pi R_0}}$$

From which we can estimate an ACC transport:

$$\text{transport} = \frac{W}{f_0}\left[\frac{\tau_x}{\rho_0 CHR_0\pi}\right]^{\frac{1}{2}}\int_{z=-H}^{0} \mathrm{d}z' \int_{z'=-H}^{0} N(z'')\mathrm{d}z''.$$

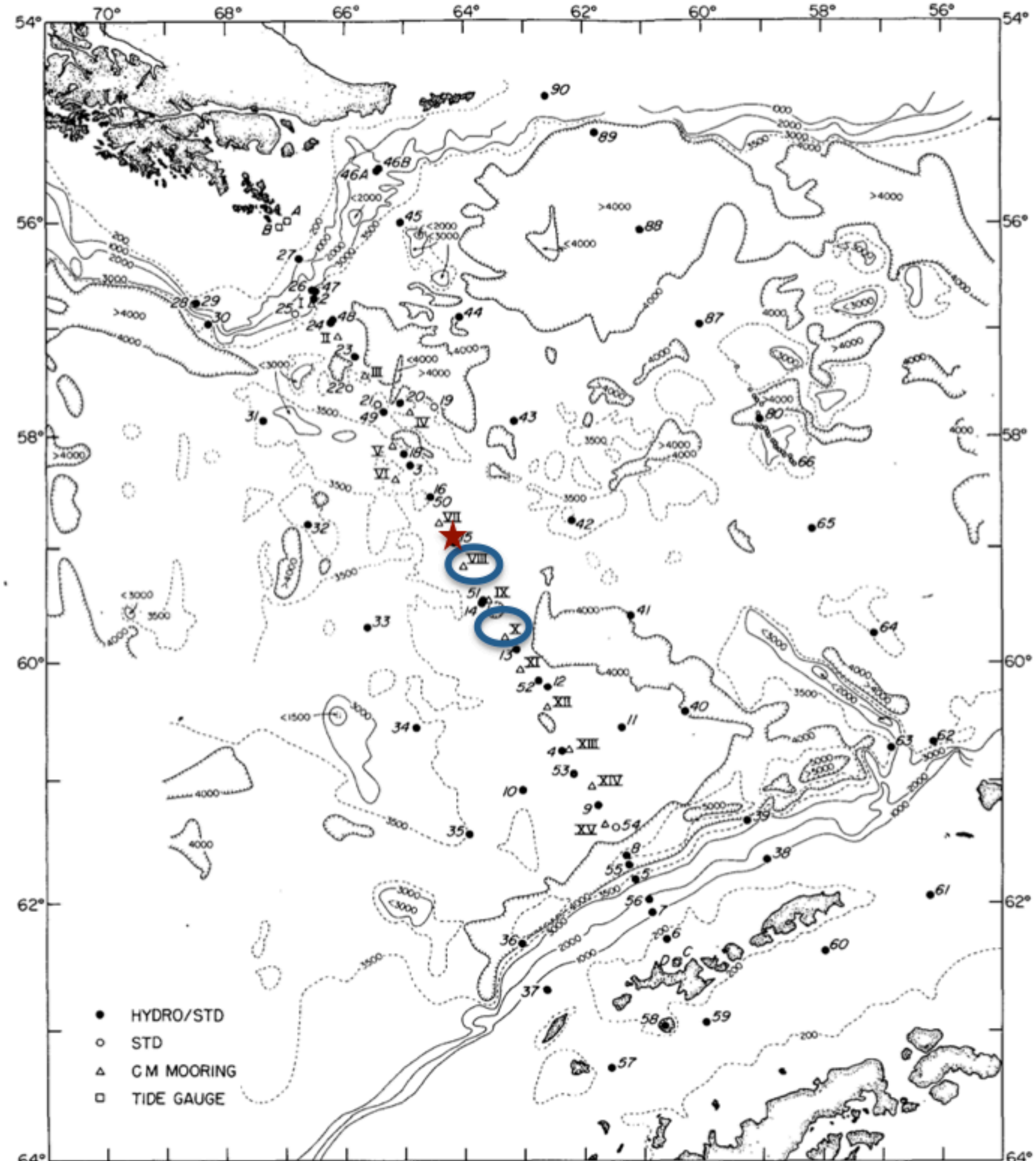

FIG. 1. *Melville* station plan, FDRAKE 75, 19 February–30 March 1975.

$$\overline{U_z}(z) = \frac{N(z)}{f}\sqrt{\frac{\tau_x}{\rho_0 C H \pi R_0}}$$

$f = -1.25 \times 10^{-4}$ 1/s
$\tau_x = 0.2$ N/m^2
$\rho_0 = 1030$ kg/m^3
$C = 0.144$ from Stone (1972)
$H = 3500$ m
$R_0 = 12.6$ km (from Drake Passage avg N^2 profile)

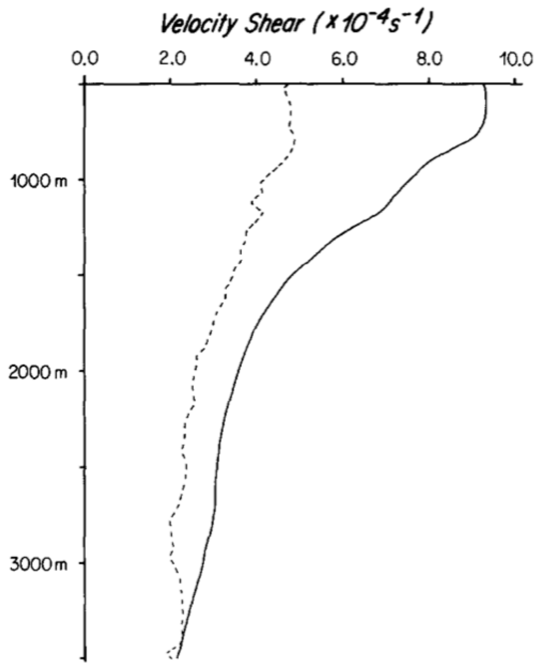

Fig. 6. Velocity shear observed in Drake Passage (solid line) plotted with velocity shear predicted by equation (7) (dashed line).

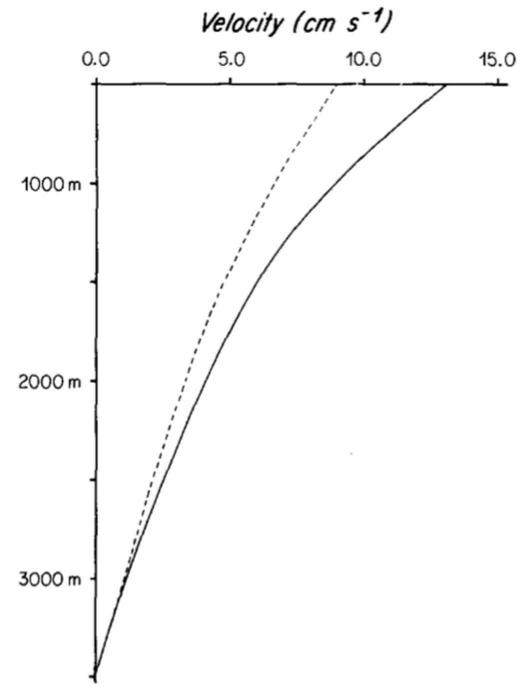

Fig. 7. Velocity referenced to 3500 m as observed in Drake Passage (solid line) vs that predicted by equation (7) (dashed line).

THE MODEL

$$\rho_0 f \frac{\overline{v'T'}}{\overline{\theta}_z} = \tau^x$$

For discussion: the authors assume that the RHS is just as evenly distributed as the LHS. Is this a reasonable assumption?

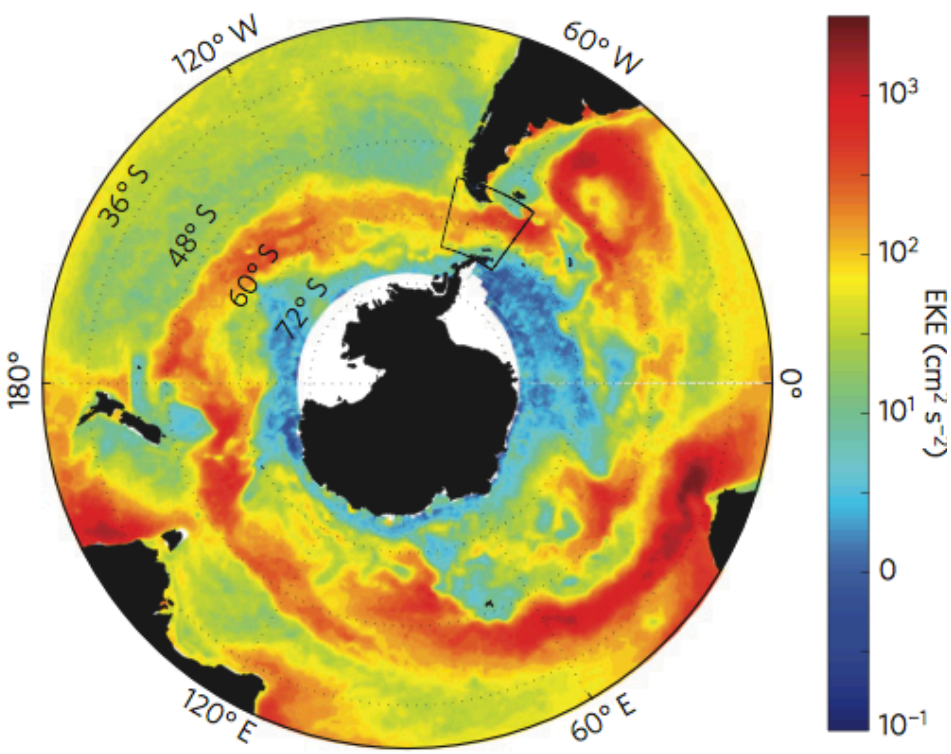

EKE from surface altimetry, 2003-2013.
Sheen et al., 2014.

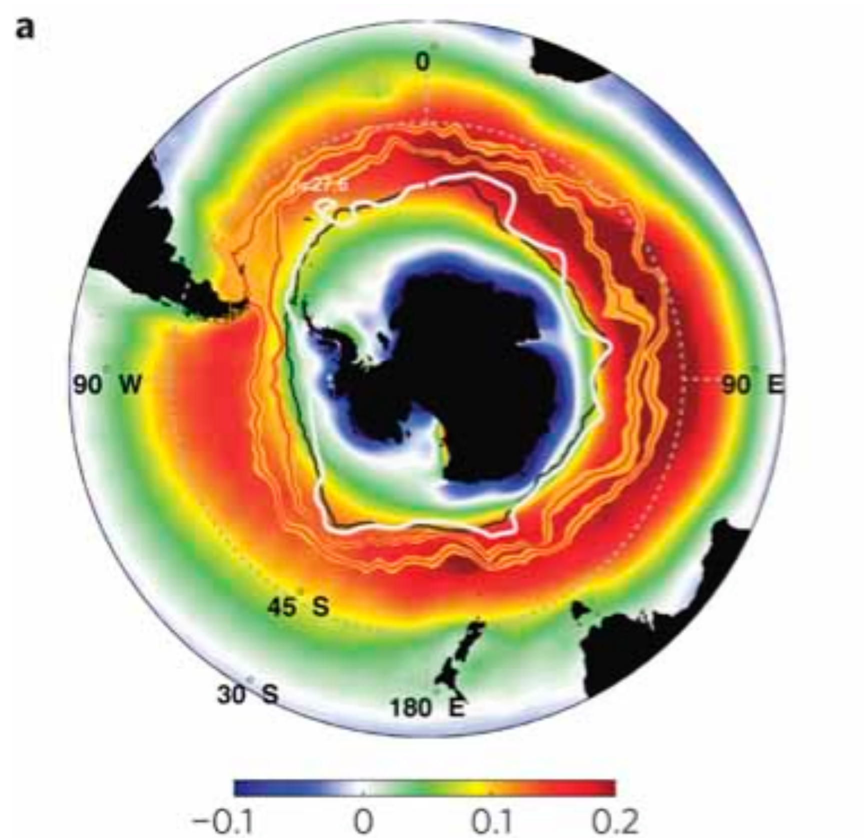

Wind stress (N/m^2) from NCEP reanalysis,
1980-2000. Marshall and Speer, 2012.

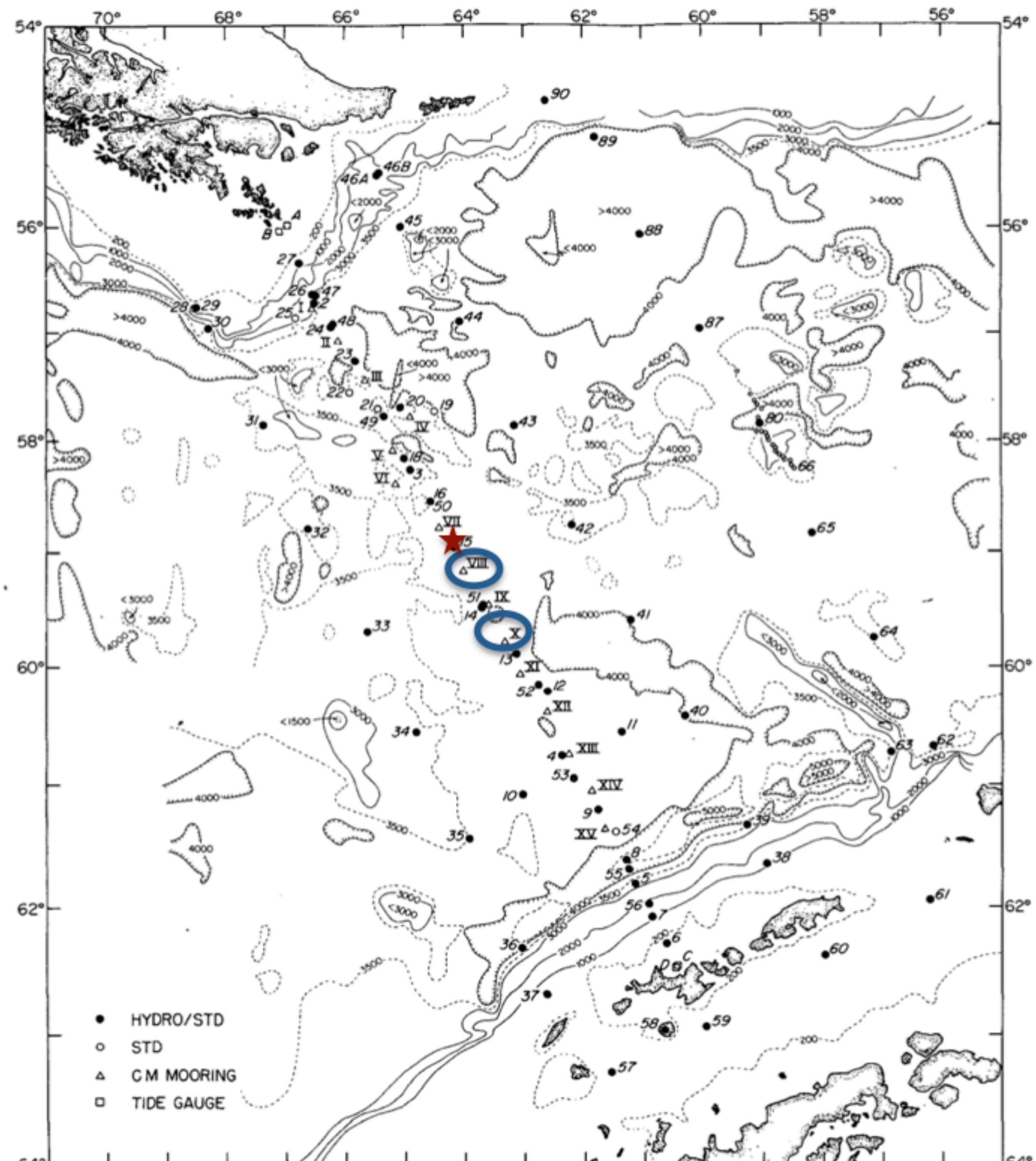

FIG. 1. *Melville* station plan, FDRAKE 75, 19 February–30 March 1975.

Zoom in to Drake Passage: cDrake Experiment, 2007-2011.

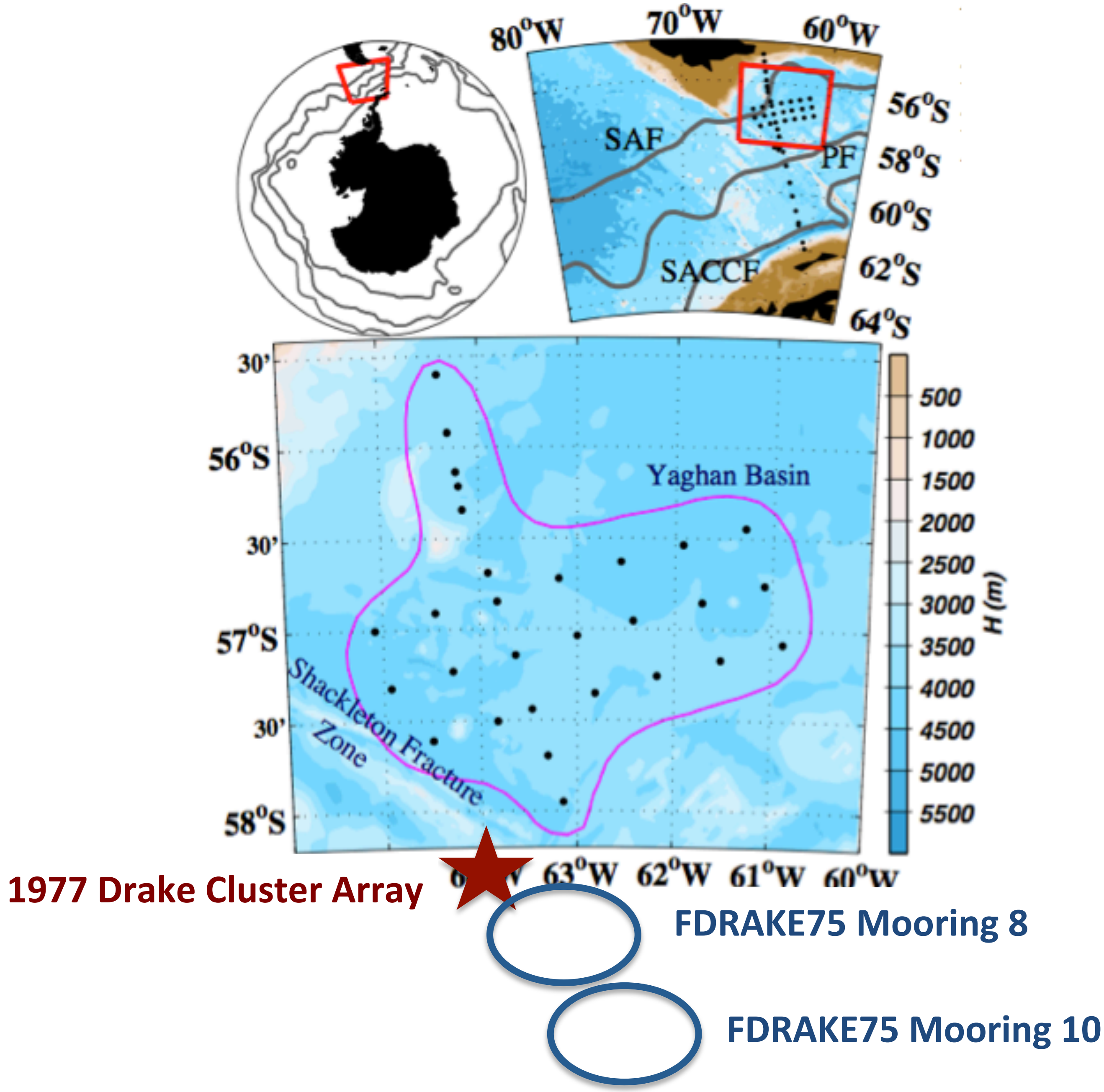

Table 1. *Eddy heat flux and downwa* ... *ds in central Drake Passage. Data used were taken in Drake Passage* ... *ata used to calculate eddy heat flux values is taken from the* 1977 *cent* ... 64°W (Bryden, 1979b), *and moorings* 8 (59°S, 64°30′W) *and* 10 (60 ... *array. Calculation of* θ_z *was performed using an arithmetic mean of* ... *d 42 taken near the moorings by the R.V.* Melville *during FDRAKE* 7 ... 25 × 10^{-4} s^{-1} (*appropriate for* 59°S) *were used. See* Nowlin et al. (19 ... *tions and moorings* 8 *and* 10

Depth (m)	Eddy heat flux $\overline{V'T'}$ (°C cm s^{-1})	Downward momentum flux $\rho_0 f\,\overline{V'T'}/\theta_z$ (dyn cm^{-2})
580*	–0.39	7.6
1020†	–0.33	7.6
1100*	–0.36	8.3
1520†	–0.32§	5.2
2080*	–0.34§	5.9
2520†	–0.24§	3.9
2750‡	–0.20	3.5
3560*	–0.18	4.3

* 1977 Drake Passage Cluster Array
† FDRAKE 75 mooring 10.
‡ FDRAKE 75 mooring 8.
§ Significantly different from zero at

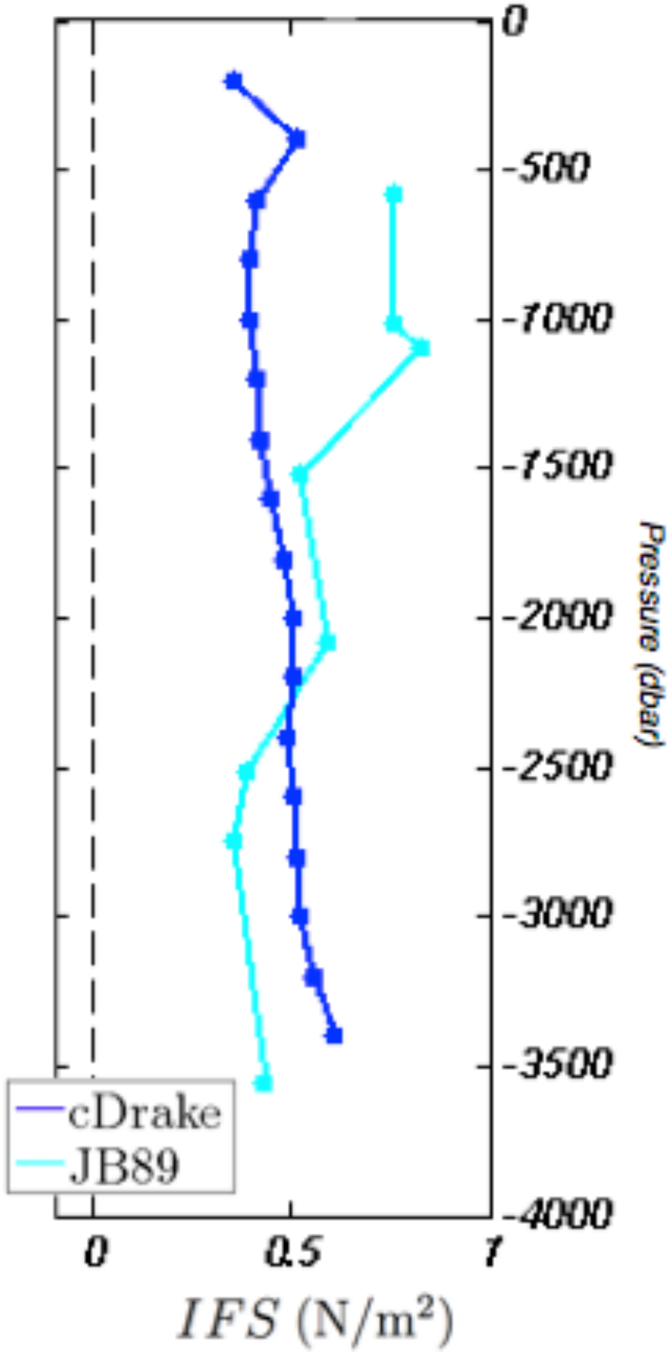

cDrake spatial and temporal variability.

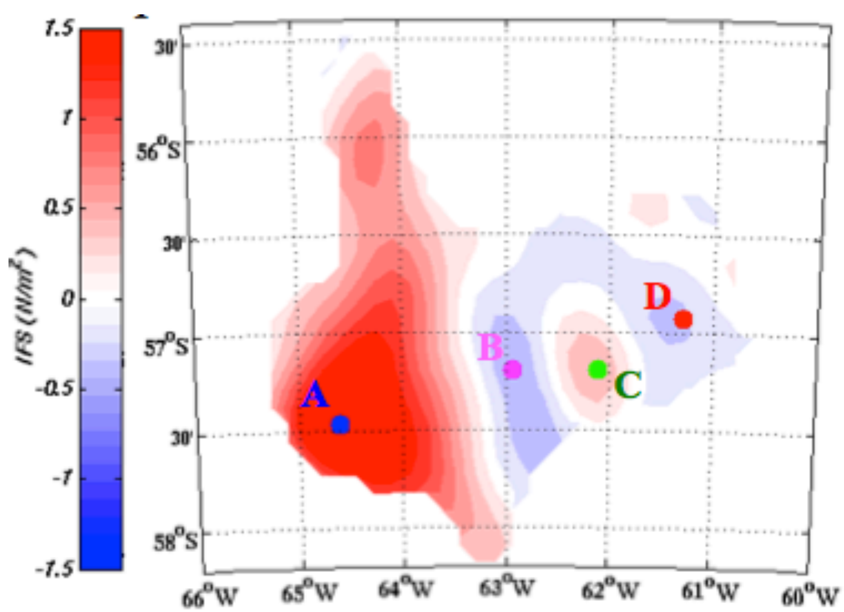

Vertical, time mean IFS.

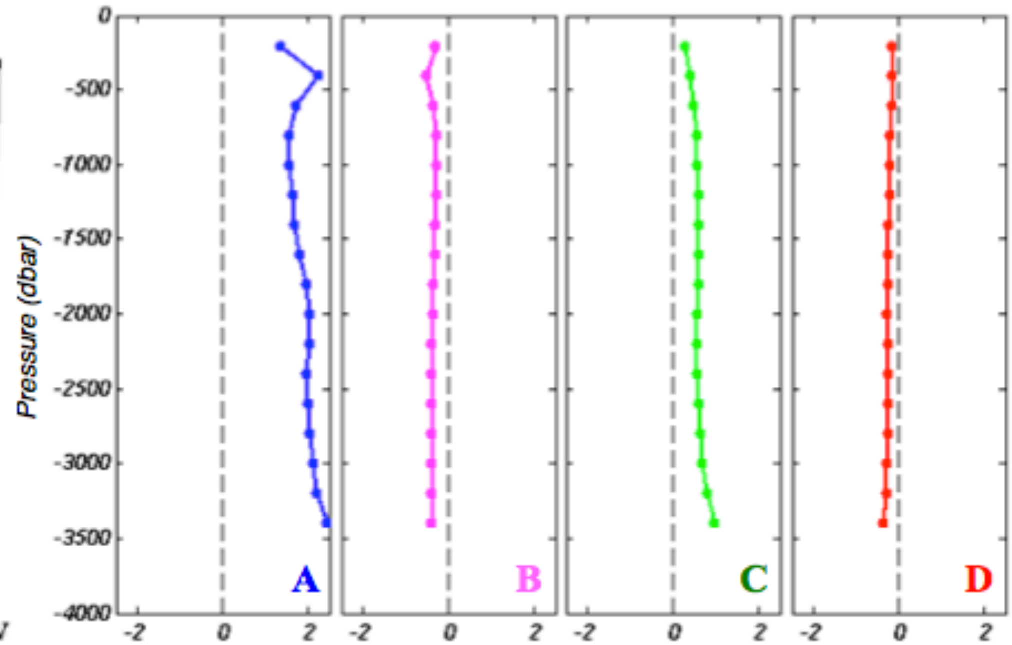

Time mean IFS profiles.